

NUMERICAL SIMULATION OF GENERALIZED NEWTONIAN AND OLDROYD-B FLUIDS FLOW

Radka Keslerová, Karel Kozel

CTU in Prague, Faculty of Mechanical Engineering,
Department of Technical Mathematics
Karlovo nám. 13, 121 35 Prague, Czech Republic
keslerov@marian.fsik.cvut.cz, Karel.Kozel@fs.cvut.cz

Abstract

This work deals with the numerical solution of generalized Newtonian and Oldroyd-B fluids flow. The governing system of equations is based on the system of balance laws for mass and momentum for incompressible laminar viscous and viscoelastic fluids. Two different definition of the stress tensor are considered. For viscous case Newtonian model is used. For the viscoelastic case Oldroyd-B model is tested. Both presented models can be generalized. In this case the viscosity is defined as a shear rate dependent viscosity function $\mu(\dot{\gamma})$. One of the most frequently used shear-thinning models is a cross model. Numerical solution of the described models is based on cell-centered finite volume method using explicit Runge Kutta time integration. The numerical results of generalized Newtonian and generalized Oldroyd-B fluids flow obtained by this method are presented and compared.

1. Mathematical model

In order to simulate the fluids flow in the channel the system of balance laws of mass and momentum for incompressible fluids are considered, [1], [4]:

$$\operatorname{div} \mathbf{u} = 0 \quad (1)$$

$$\rho \frac{\partial \mathbf{u}}{\partial t} + \rho(\mathbf{u} \cdot \nabla) \mathbf{u} = -\nabla P + \operatorname{div} \mathbf{T} \quad (2)$$

where P is the pressure, ρ is the constant density, \mathbf{u} is the velocity vector, $\mathbf{u} = (u, v, w)^T$. The symbol \mathbf{T} represents the stress tensor.

1.1. Stress tensor

In this work the different definition of the stress tensor are used.

In the case of viscous fluids the used model corresponding to Newtonian fluid is *Newtonian model*:

$$\mathbf{T} = 2\mu \mathbf{D} \quad (3)$$

where μ is dynamic viscosity and tensor \mathbf{D} is symmetric part of the velocity gradient defined by the relation $\mathbf{D} = \frac{1}{2}(\nabla\mathbf{u} + \nabla\mathbf{u}^T)$.

If viscoelastic fluids are considered *Maxwell model* as the simplest viscoelastic model is used:

$$\mathbf{T} + \lambda_1 \frac{\delta\mathbf{T}}{\delta t} = 2\mu\mathbf{D} \quad (4)$$

where λ_1 has dimension of time and denotes the relaxation time. The symbol $\frac{\delta}{\delta t}$ represents upper convected derivative (see (8))

By combination of these two models the behaviour of mixture of viscous and viscoelastic fluids can be described. Such a model is called *Oldroyd-B model* and it has the form

$$\mathbf{T} + \lambda_1 \frac{\delta\mathbf{T}}{\delta t} = 2\mu \left(\mathbf{D} + \lambda_2 \frac{\delta\mathbf{D}}{\delta t} \right) \quad (5)$$

the parameters λ_1, λ_2 are relaxation and retardation time.

The stress tensor \mathbf{T} can be decomposed to the Newtonian part \mathbf{T}_s and viscoelastic part \mathbf{T}_e ($\mathbf{T} = \mathbf{T}_s + \mathbf{T}_e$) and

$$\mathbf{T}_s = 2\mu_s\mathbf{D}, \quad \mathbf{T}_e + \lambda_1 \frac{\delta\mathbf{T}_e}{\delta t} = 2\mu_e\mathbf{D}, \quad (6)$$

where

$$\frac{\lambda_2}{\lambda_1} = \frac{\mu_s}{\mu_s + \mu_e}, \quad \mu = \mu_s + \mu_e. \quad (7)$$

The upper convected derivative $\frac{\delta}{\delta t}$ is defined (for general tensor \mathbf{M}) by the relation (see [2])

$$\frac{\delta\mathbf{M}}{\delta t} = \frac{\partial\mathbf{M}}{\partial t} + (\mathbf{u}\cdot\nabla)\mathbf{M} - (\mathbf{W}\mathbf{M} - \mathbf{M}\mathbf{W}) - (\mathbf{D}\mathbf{M} + \mathbf{M}\mathbf{D}) \quad (8)$$

where \mathbf{D} is symmetric part of the velocity gradient

$$\mathbf{D} = \frac{1}{2}(\nabla\mathbf{u} + \nabla\mathbf{u}^T) = \frac{1}{2} \begin{pmatrix} 2u_x & u_y + v_x & u_z + w_x \\ u_y + v_x & 2v_y & v_z + w_y \\ w_x + u_z & w_y + v_z & 2w_z \end{pmatrix} \quad (9)$$

and \mathbf{W} is antisymmetric part of the velocity gradient

$$\mathbf{W} = \frac{1}{2}(\nabla\mathbf{u} - \nabla\mathbf{u}^T) = \frac{1}{2} \begin{pmatrix} 0 & u_y - v_x & u_z - w_x \\ v_x - u_y & 0 & v_z - w_y \\ w_x - u_z & w_y - v_z & 0 \end{pmatrix}. \quad (10)$$

The governing system (1), (2) of equations is completed by the equation for the viscoelastic part of the stress tensor

$$\frac{\partial\mathbf{T}_e}{\partial t} + (\mathbf{u}\cdot\nabla)\mathbf{T}_e = \frac{2\mu_e}{\lambda_1}\mathbf{D} - \frac{1}{\lambda_1}\mathbf{T}_e + (\mathbf{W}\mathbf{T}_e - \mathbf{T}_e\mathbf{W}) + (\mathbf{D}\mathbf{T}_e + \mathbf{T}_e\mathbf{D}). \quad (11)$$

Both models could be generalized. In this case the viscosity μ is no more constant, but is defined by viscosity function according to the cross model (for more details see [11])

$$\mu(\dot{\gamma}) = \mu_\infty + \frac{\mu_0 - \mu_\infty}{(1 + (\lambda\dot{\gamma})^b)^a} \quad (12)$$

where

$$\dot{\gamma} = 2\sqrt{\frac{1}{2}\text{tr } \mathbf{D}^2} \quad (13)$$

$$\begin{aligned} \mu_0 &= 1.6 \cdot 10^{-1} Pa \cdot s & \mu_\infty &= 3.6 \cdot 10^{-3} Pa \cdot s \\ a &= 1.23, b = 0.64 & \lambda &= 8.2s. \end{aligned}$$

2. Numerical solution

In this work the steady state solution is considered. In this case an artificial compressibility method can be applied. It means that the continuity equation is completed by the time derivative of the pressure in the form (for more details see e.g. [3], [8]):

$$\frac{1}{\beta^2} \frac{\partial p}{\partial t} + \text{div } \mathbf{u} = 0, \quad \beta \in \mathbb{R}^+. \quad (14)$$

The system of equations (including the modified continuity equation) could be rewritten in the conservative form.

$$\tilde{R}_\beta W_t + F_x^c + G_y^c + H_z^c = F_x^v + G_y^v + H_z^v + S, \quad \tilde{R}_\beta = \text{diag}\left(\frac{1}{\beta^2}, 1, \dots, 1\right) \quad (15)$$

where W is the vector of unknowns, F^c, G^c, H^c are inviscid fluxes, F^v, G^v, H^v are viscous fluxes, and the source term S .

The following special parameters settings related to four specific models will be used in our numerical simulation:

Newtonian	$\mu(\dot{\gamma}) = \mu_s = \text{const.}$	$\mathbf{T}_e \equiv 0$
Generalized Newtonian	$\mu(\dot{\gamma})$	$\mathbf{T}_e \equiv 0$
Oldroyd-B	$\mu(\dot{\gamma}) = \mu_s = \text{const.}$	\mathbf{T}_e
Generalized Oldroyd-B	$\mu(\dot{\gamma})$	\mathbf{T}_e

The (15) is discretized in space by the cell-centered finite volume method (see [7]) and the arising system of ODEs is integrated in time by the explicit multistage Runge–Kutta scheme (see [8], [10], [11]).

2.1. Boundary conditions

The flow is modelled in a bounded computational domain where a boundary is divided into three mutually disjoint parts: a solid wall, an outlet and an inlet. At the inlet Dirichlet boundary condition for velocity vector is used and for a pressure and the stress tensor Neumann boundary condition is used. At the outlet the pressure

value is given and for the velocity vector and the stress tensor Neumann boundary condition is used. The homogeneous Dirichlet boundary condition for the velocity vector is used on the wall. For the pressure and stress tensor Neumann boundary condition is considered.

3. Numerical results

This section deals with the comparison of the numerical results of Newtonian and Oldroyd-B fluids. Numerical tests are performed in an idealized stenosed vessel. The stenosed vessel is assumed to be three-dimensional with circular cross-section. Figure 3 shows the shape of the tested domain. The computational domain is discretized using a structured, wall fitted mesh with hexahedral cells and uniform axial cell spacing. The similar numerical results can be found in [1], [2].

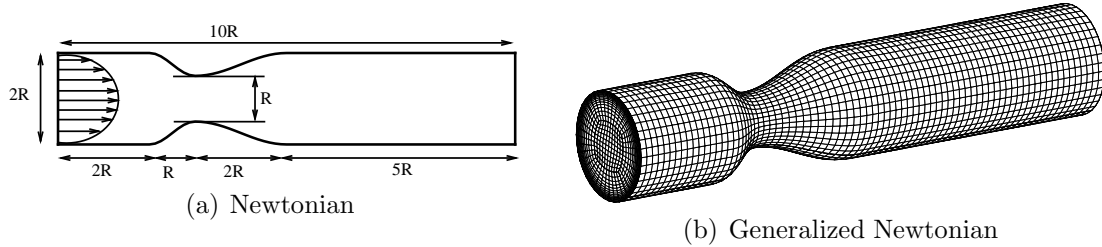


Figure 1: Structure of the computational domain.

The following model parameters are:

$$\begin{aligned}
 \mu_e &= 4.0 \cdot 10^{-4} Pa \cdot s & \mu_s &= 3.6 \cdot 10^{-3} Pa \cdot s \\
 \lambda_1 &= 0.06s & \lambda_2 &= 0.054s \\
 U_0 &= 0.0615m \cdot s^{-1} & L_0 &= 2R = 0.0062m \\
 \mu_0 &= \mu = \mu_s + \mu_e & \rho &= 1050kg \cdot m^{-3}
 \end{aligned}$$

Note that the fluid motion can be characterized by parameters: Reynolds number and Weissenberg number. Weissenberg number is proportional to the relaxation time of the fluid. These special data corresponds to Reynolds and Weissenberg numbers:

$$Re = \frac{\rho U_0 L_0}{\mu_0} = 100, \quad We = \frac{\lambda_1 U_0}{L_0} = 0.6 \quad (16)$$

In Figure 2 the comparison of the axial velocity isolines is presented. To emphasize the flow separation behind the stenosis the regions of reversal flow (with respect to axial direction) are marked with white color.

Pressure and velocity distribution along the axis for both tested fluids models is shown in Figure 3. By simple observation one can conclude that the main effect of the Oldroyd-B fluids behavior is visible mainly in the recirculation zone.

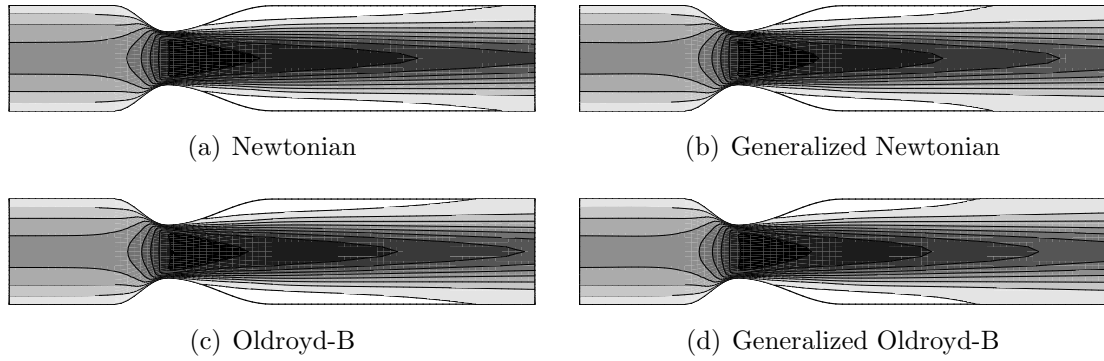


Figure 2: Axial velocity isolines for generalized Oldroyd-B fluids.

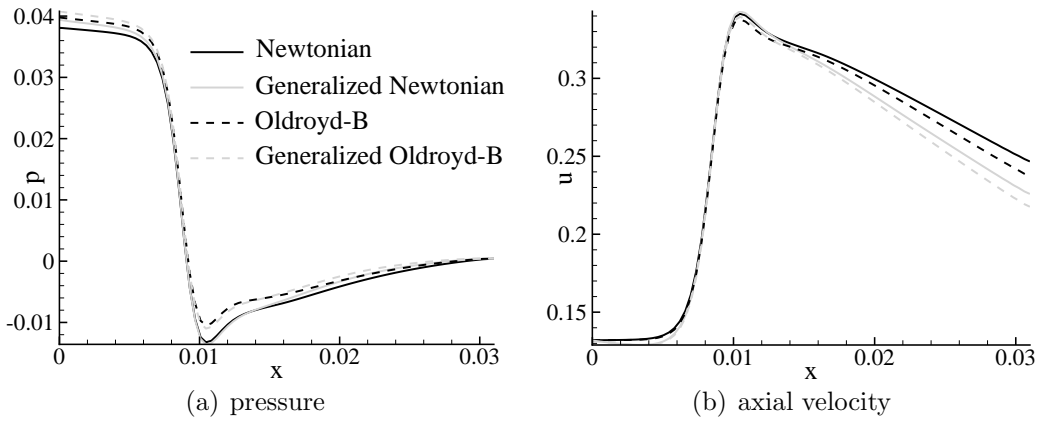


Figure 3: Pressure and axial velocity distribution along the central axis of the channel.

4. Conclusions

Newtonian and Oldroyd-B models with their generalized modification have been considered for numerical simulation of fluids flow in the idealized axisymmetric stenosis. The cell-centered finite volume solver for incompressible laminar viscous and viscoelastic fluids flow has been described. For time integration the explicit Runge–Kutta method was considered. The numerical results obtained by this method are presented. The differences between these tested fluids are given mainly in the separation region. These results clearly show that for shear-thinning flows the recirculation zone becomes shorter. This could be explained by the specific choice of the characteristic viscosity μ_∞ for the reference Newtonian and (non-generalized) Oldroyd-B solution.

Acknowledgements

This work was partly supported by the grant GACR P201/11/1304 and GACR 201/09/0917.

References

- [1] Bodnar, T., Sequeira, A., and Prosi, M.: On the shear-thinning and viscoelastic effects of blood flow under various flow rates. *Appl. Math. Comput.* **217** (2011), 5055–5067.
- [2] Bodnar, T. and Sequeira, A.: Numerical study of the significance of the non-Newtonian nature of blood in steady flow through stenosed vessel. In: R. Rannacher, A. Sequeira (Eds.), *Advances in Mathematical Fluid Mechanics*, pp. 83–104. Springer-Verlag, 2010.
- [3] Chorin, A. J.: A numerical method for solving incompressible viscous flow problem. *J. Comput. Phys.* **135** (1967) 118–125.
- [4] Dvořák, R. and Kozel, K.: *Mathematical modelling in aerodynamics (in Czech)*. CTU, Prague, Czech Republic, 1996.
- [5] Gaitonde, A. L.: A dual-time method for two dimensional unsteady incompressible flow calculations. *International Journal for Numerical Methods in Engineering.* **41** (1998), 1153–1166.
- [6] Keslerová, R. and Kozel, K.: Numerical modelling of incompressible flows for Newtonian and non-Newtonian fluids. *Math. Comput. Simulation* **80** (2010), 1783–1794.
- [7] LeVeque, R.: *Finite-volume methods for hyperbolic problems*. Cambridge University Press, 2004.
- [8] Keslerová, R. and Kozel, K.: Numerical modelling of incompressible flows for Newtonian and non-Newtonian fluids. *Math. Comput. Simulation* **80** (2010), 1783–1794.
- [9] Robertson, A.M., Sequeira, A., and Kameneva, M.V.: *Hemorheology*. Birkhäuser Verlag Basel, Switzerland, 2008.
- [10] Jameson, A., Schmidt, W., and Turkel, E.: Numerical solution of the Euler equations by finite volume methods using Runge-Kutta time-stepping schemes. AIAA 14th Fluid and Plasma Dynamic Conference California, 1981.
- [11] Vimmr, J. and Jonášová, A.: Non-Newtonian effects of blood flow in complete coronary and femoral bypasses. *Math. Comput. Simulation* **80** (2010), 1324–1336.